J Solid State Electrochem (2000) 4: 425–434

ORIGINAL PAPER

J.A. Weima · A.M. Zaitsev · R. Job · G. Kosaca
F. Blum · G. Grabosch · W.R. Fahrner · J. Knopp

Investigation of non-diamond carbon phases and optical centers in thermochemically polished polycrystalline CVD diamond films

Received: 26 July 1999 / Accepted: 15 November 1999

Abstract Polycrystalline chemical vapor deposition (CVD) diamonds films grown on silicon substrates using the microwave-enhanced CVD technique were polished using the thermochemical polishing method. The surface morphology of the samples was determined by optical and scanning electron microscopes before and after polishing. The average surface roughness of the as-grown films determined by the stylus profilometer yielded 25 μm on the growth side and about 7 μm on the substrate side. These figures were almost uniform for all the samples investigated. Atom force microscopic measurements performed on the surface to determine the average surface roughness showed that thermochemical polishing at temperatures between 700 °C and 900 °C reduced the roughness to about 2.2 nm on both the substrate and growth sides of the films. Measurements done at intermittent stages of polishing using confocal micro-Raman spectroscopy showed that thermochemical polishing is accompanied by the establishment of non-diamond carbon phases at 1353 cm^{-1} and 1453 cm^{-1} at the initial stage of polishing and 1580 cm^{-1} at the intermediate stage of polishing. The non-diamond phases vanish after final fine polishing at moderate temperatures and pressures. Photoluminescence of defect centers determined by an Ar^{+} laser ($\lambda l_{exct} =$ 514.532 nm) showed that nitrogen-related centers with two zero-phonon lines at 2.156 eV and 1.945 eV and a silicon-related center with a zero-phonon line at 1.681 eV are the only detectable defects in the samples.

J.A. Weima (✉) · A.M. Zaitsev · R. Job · G. Kosaca
F. Blum · G. Grabosch · W.R. Fahrner
Department of Electronic Devices,
Faculty of Electrical Engineering,
University of Hagen, Haldener Strasse 182,
58084 Hagen, Germany

J. Knopp
Fries Research and Technology GmbH,
Friedrich-Ebert-Strasse, 51429 Bergisch-Gladbach,
Germany

Key words Thermochemical polishing · Diamond films · Non-diamond phases · Defects · Atomic force microscopy

Introduction

Polycrystalline chemical vapor deposition (CVD) diamond films have found a wide range of applications in several fields of research and there is an ever-increasing demand for ultra-smooth surface processing that could enhance the efficiency of such applications. Diamond films which find use in the making of heat sinks, optical windows, electronic sensors, etc., require ultra-precise surface polishing. Such smooth surfaces facilitate firm electrical contacts necessary for the manufacturing of electronic devices on diamond substrates.

A significant amount of work has been expended on a wide range of methods geared towards obtaining mirror-like polished polycrystalline diamond surfaces [1–5]. These methods, however, are not without shortcomings, some of which may negatively affect the polishing quality of CVD diamond films considerably. As a result of the random orientation of the crystallites building up the films, polishing becomes exceptionally difficult using conventional methods. These are sensitive to directional and planar random orientations of the crystallites constituting the films. Previous researchers [5] have shown that effective polishing is hard to attain in the (111) planes and [111] directions of the diamond films. Thus reasonable polishing in such planes and directions requires a lot of time when conventional polishing methods are employed.

Mechanical polishing [5] has been used quite often as a conventional method of polishing CVD diamonds. The limitations to this polishing method are many and grave. The use of a heavy weight on the diamond sample during polishing causes damage to the lattice structures of the film and can lead to increasing mechanical streses within the films. The chipping of small particles from the polishing surface worsens the polishing quality to an

extent that the surface roughness attained after polishing is still in the proximity of several nanometers. Alternatives to mechanical polishing such as solid oxidizers [6] have been used to etch diamond surfaces at temperatures in the neighborhood of 700 K. The average roughnesses of large area polished films have been thinned down to about 5 nm using this method. However, polishing is restricted only to conductive diamond films. Chemo-mechanical polishing [7] with KNO_3 has been used to reduce the average surface roughness of diamond films to less than 1 nm. This polishing quality, however, was attained only on (100) diamond surfaces which are most easy to polish. Thus, the chemo-mechanical polishing method has not yet manifested its efficiency with regard to polishing polycrystalline diamond films of varying orientations and crystal structures.

An effective way of overcoming the limitations imposed by the above methods has been achieved through the advent of the thermochemical polishing technique. The polishing of polycrystalline diamond films has been successfully done on both small and large area CVD diamond films without encountering difficulties in defined directions or planes [4]. Unlike the mechanical polishing technique which employs heavy weights, the application of light weights on the diamond films during thermochemical polishing ensures that the surfaces remain undamaged after the polishing process. The thermochemical polishing method has been used to effectively and sufficiently thin down the surface roughness of polycrystalline diamond films to a few nanometers. The experimental setup is simple to construct, less expensive, and achieves ultra-precise polishing in a short period of time. The mechanism of polishing has been described by previous researchers [8–14]. Accelerated polishing of film surfaces is acquired through the use of hydrogen as the ambient atmosphere. The selection of hydrogen as the ambient atmosphere lies in its capability to interact with carbon atoms and eventually form methane gas as a product of the chemical reaction between the constituent elements.

The objective of this work is to present the results obtained through thermochemical polishing of CVD polycrystalline diamond films. Confocal micro-Raman spectroscopy was used to optically characterize the films at intermittent stages of polishing. The thermochemical polishing enhanced transformation of diamond into non-diamond phases is discussed. Photoluminescence and depth distribution of defect centers in the films are also discussed.

Experimental

Figure 1 shows a schematic cross-section of the thermochemical polishing apparatus used in the polishing of the polycrystalline CVD diamond films. The CVD diamond sample is placed between

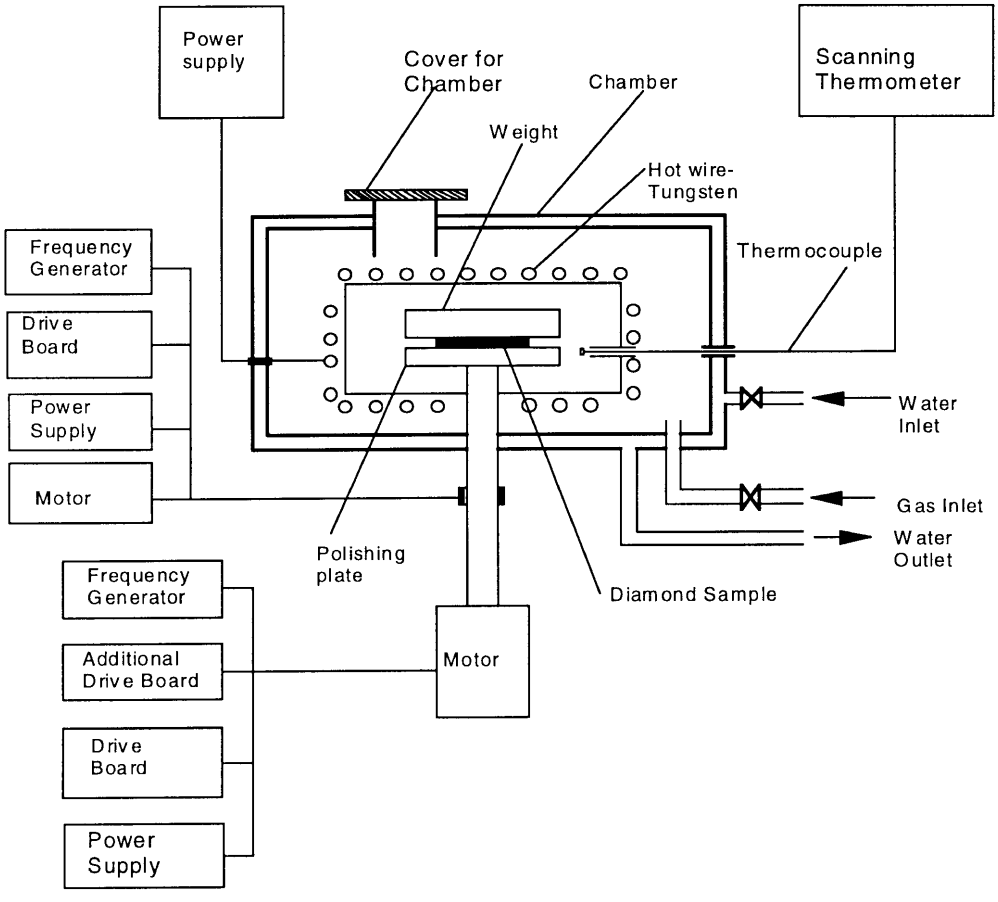

Fig. 1 Experimental set-up of the thermochemical polishing apparatus

the polishing plate and the weight. The polishing plate is driven by a step motor which receives rectangular positive pulses from the drive board through the frequency generator. The additional drive board provides a dual means of rotating the polishing plate. It ensures a continuous one-directional rotation covering 200 steps per revolution on one the hand, and a two-step forward, one-step backwards motion on the other hand. This is done by simply selecting the appropriate switch. The velocity of the polishing plate can be regulated by selecting the desired frequency from the frequency generator.

An additional step motor was included to produce transversal vibrations that tear the polishing plate from the sample, thus reducing the frictional force between the two. The transversal vibrations also ensure that the upper weight, which is meant to press the diamond film firmly against the polishing plate, does not rotate during the polishing process. This effectuates the simultaneous polishing of both sides of the sample. The vibrational step motor is programmed to produce to-fro half-step vibrations, two half-step vibrations, three half-step vibrations, and four half-step vibrations as required. In this way, the amplitude of the vibrations can be selected at will. The frequency generator for this motor can operate at 100–1800 Hz. The ambient atmosphere used in the experiments is a gas mixture comprising 4% hydrogen and 96% argon. The gas mixture replaces the oxygen in the chamber and hence prevents oxidation of the diamond film at high temperatures. Polishing was done at temperatures of 700–900 °C. The angular velocity of the polishing plate ranged between 0.5 revolutions per second and 3.0 revolutions per second. This was achieved by selecting the appropriate frequency from the frequency generator. The power supply heats the spiral tungsten wire surrounding the polishing plate and the temperature in the chamber is measured by a scanning thermometer via a thermocouple. The gas pressure in the chamber should be slightly above atmospheric pressure so that air from outside does not rush in during polishing. The outer chamber is continuously cooled with water to keep it in thermal equilibrium with the outside surroundings.

The mechanism involving the catalysis of the diamond-metal reaction during thermochemical polishing has been discussed earlier [4, 13, 14]. The principle is based on the conversion of diamond into non-diamond phases at high temperatures under catalytic action of a transition metal and the subsequent dissolution of the carbon atoms into the metal. Iron, which has a high coefficient of diffusion for carbon, is also known to offer a carbon solubility of about 170 mg cm^{-3} at eutectic temperatures. Undoubtedly, iron is one of the most suitable transitional metals to be used as a polishing plate. The initial concentration of carbon in the polishing plate influences the carbon diffusion. Hence it influences the removal rate. Saturation of the surface of the polishing plate with carbon atoms retards the rate of diffusion [4]. It is therefore necessary to change the polishing plate intermittently or to remove at least 0.5 mm of the surface of the polishing plate after using it for a period of about 24 h to avoid the saturation effect. The polishing plates used in the experiments had a diameter of 18.0 mm and a thickness of 12 mm. Thick polishing plates of this sort are preferable because they ensure that the carbon atoms get deep down into the metal, thereby averting their accumulation and saturation on the surface of the polishing plate.

The removal rate is influenced profoundly by the degree of contact between the polishing plate and the diamond film. At the initial stage of polishing, when only a few carbon atoms are involved in establishing contact between the plate and the diamond film, the removal rate is enhanced by the conversion of diamond into non-diamond carbon, and diffusion into the polishing plate is low [4]. This phenomenon is confirmed by the existence of thin layers of non-diamond carbon phases on the surface of both the diamond film and the polishing plate. As the contact between the plate and the diamond film increases, the process of diffusion supersedes and the polishing process is accelerated by the dissolution of carbon atoms into the polishing plate [4].

Results and discussion

Figure 2a shows an optical micrograph of the growth side of an as-grown polycrystalline CVD diamond film magnified 400 times. The random orientation of the crystallite constituting the film is clearly seen. The sizes of the crystallites range between 5 μm and 40 μm. The bright spots on the micrograph represent crystallites lying on the upper surface of the film, while the darker spots show low-lying crystallites.

The average surface roughness of the growth side of the as-grown films yielded 25 μm after measuring with the stylus profilometer. Figure 2b is the optical micrograph of the substrate side of the same film. Bright and dark spots could be seen on the micrograph, signifying that the substrate side is also not smooth although it is free from large crystallites. The average surface roughness of the substrate side was found to be about 7 μm.

Figure 3a is the optical micrograph of the growth side of a thermochemically polished polycrystalline CVD diamond film. Figure 3b is the optical micrograph of the substrate side of the same film. The magnification was 2000 times in both cases. With the exception of very tiny hole-like features on the polished films, the surfaces are well polished and the surface roughness of the film as measured by the stylus profilometer were found to be 1.7 nm on the growth side and 1.3 nm on the substrate side. The origin of the hole-like features seen on the polished surface could be a characteristic of the diamond films rather than an effect originating from the thermochemical polishing method itself. Surface roughness measured by the stylus profilometer is often not without error, especially when the peaks and valleys summing up the surface roughness are below the dimensions of the tip of the profilometer [15]. The tip of the profilometer used in these measurements had a diameter of 5 μm. It can be stated with certainty that the tip of this profilometer is fairly large and measurement of surface roughnesses to a few nanometers cannot be done without considerable error. The surfaces of the polished films were therefore further investigated by the atom force microscope (AFM), which has a better resolution than the stylus profilometer [15, 16].

The images of the AFM measurements are shown in Fig. 4a and b for the growth and substrate sides of a polished CVD diamond film, respectively. The AFM-measured average surface roughness 2.2 nm on the growth side of this diamond film was and 2.1 nm on the substrate side. Thus, the initial roughness of both sides of the film has been reduced by almost four orders of magnitude after thermochemical polishing. The two surfaces of the film were polished down to almost the same quality. It should be noted that, in comparison with earlier results [4], the ultra-smooth polishing achieved on the substrate side was a result of the additional step motor included in the construction of the polishing apparatus. The transverse vibrations produced by this motor ensured that the weight placed on the

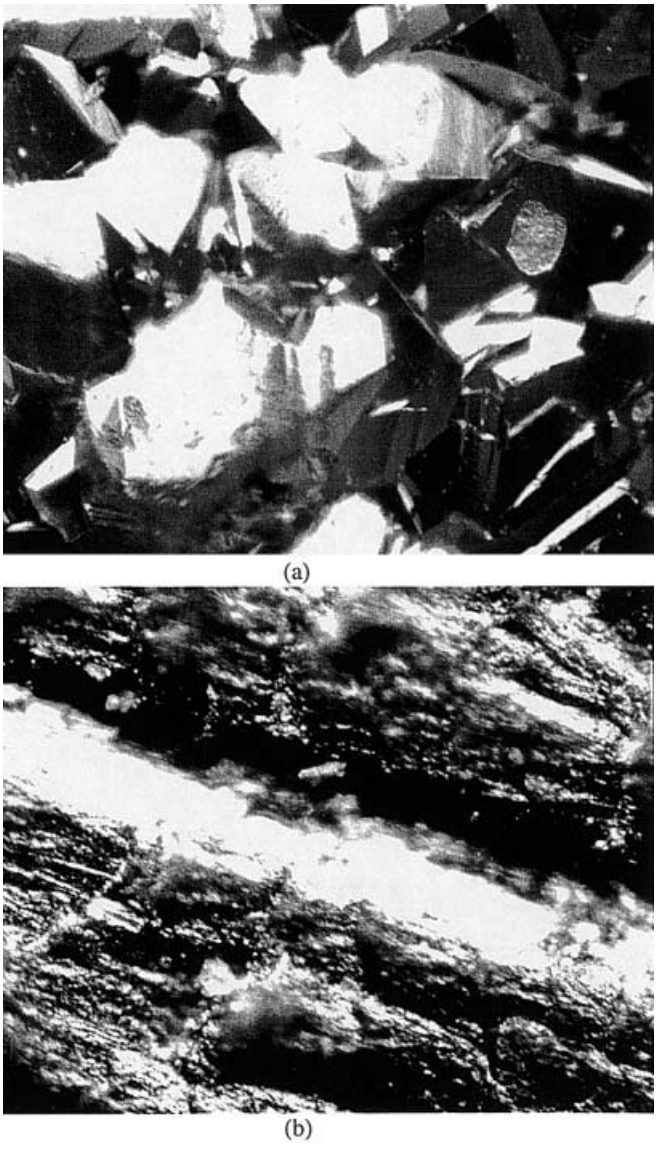

Fig. 2 **a** Optical micrograph of an as-grown polycrystalline CVD diamond film magnified 400 times. **b** The substrate side of the same film in **a** also magnified 400 times

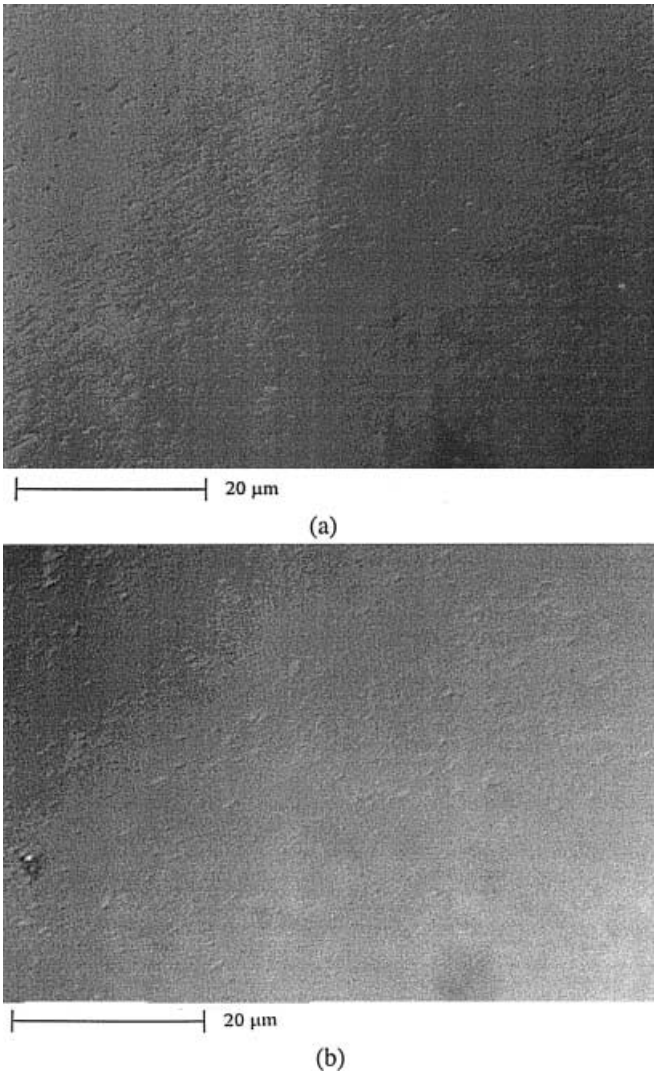

Fig. 3 **a** Optical micrograph of the growth side of a thermochemically polished polycrystalline CVD diamond film. **b** The substrate side of the same film in **a** after thermochemical polishing. Both sides are magnified 2000 times

diamond film to maintain contact between the polishing plate and the film did not rotate during polishing, so that the substrate side of the film was polished simultaneously with the growth side. The upper weight is in effect a polishing plate with the same polishing capability as the main polishing plate. The upper weight and the polishing plate are made of steel with a low carbon content.

The Dilor Micro-Raman system has been used to investigate the constituents of the non-diamond carbon at intermittent stages of polishing. An argon ion laser with an excitation line at 514.532 nm and an output power ranging between 15 and 20 mW was used as the excitation source. The Raman measurements were done at room temperature.

Figure 5a–f shows the Raman spectra of an as-grown CVD diamond film before and during various stages of thermochemical polishing. The spectrum of the as-grown film in Fig. 5a exhibits a small band at 1205 cm^{-1} and a broad band extending from 1350 cm^{-1} to about 1555 cm^{-1}. Previous researchers have attributed the existence of the peak at 1205 cm^{-1} to mixed bonds arising between sp^2 and sp^3 bonded carbon systems [17]. The broad band could not be associated with any peak, but it covers a region where two peaks are normally seen. It could therefore be attributed to a joint band comprising disordered (nanocrystalline) graphite with a peak around 1353 cm^{-1} and the amorphous diamond-like carbon with a peak around 1455 cm^{-1} [18, 19]. Since this band is seen in the as-grown film, it is obvious that these phases are incorporated in the diamond film during CVD. The spectrum was taken at a spot very close to the grain boundary. It has been shown that grain boundaries are filled with non-diamond carbon in the form of graphite [20]. Spectra of as-grown diamonds taken at the grain center are usually free of non-diamond carbon

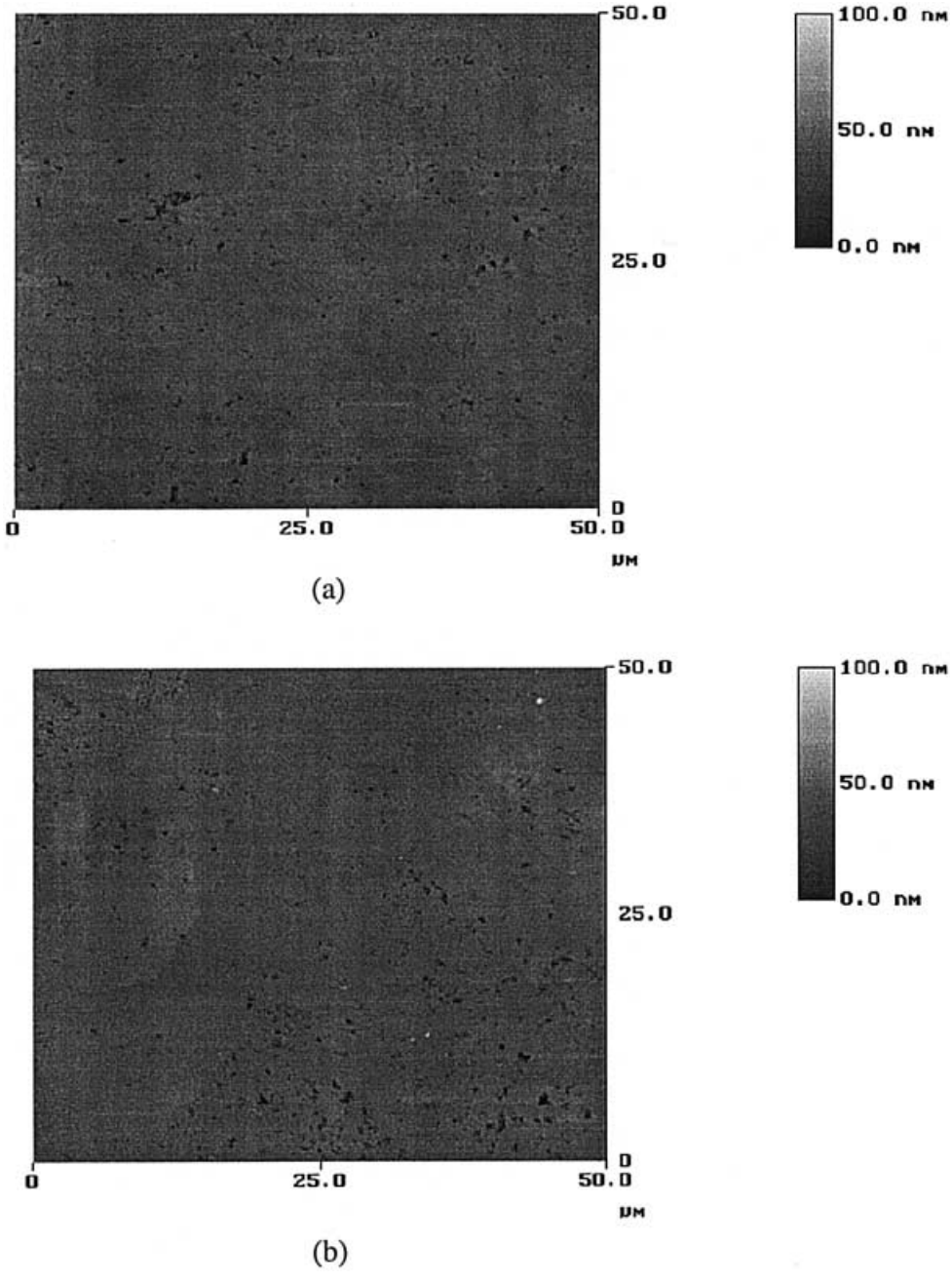

Fig. 4 **a** AFM image of the growth side of a polished CVD diamond film. **b** AFM image of the substrate side of the same film as in **a**

phases. Figure 5b shows the spectrum of the film after undergoing thermochemical polishing for 16 h. The broad peak in Fig. 5a is now seen to split into the constituent two peaks. This feature was reproducible even with spectra taken at different spots on the surface of the film. The nanocrystalline graphite band now seen at 1353 cm^{-1} is a result of disordered sp^2 bonding, while the amorphous band at 1453 cm^{-1} is related to a disordered sp^3 bonded portion of the film. Further polishing (Fig. 5c) showed an additional band at about 1580 cm^{-1}. This band has been designated to microcrystalline graphite resulting from well-ordered sp^2 bonding [17–21]. The disordered graphite and the amorphous diamond-like carbon bands are now much narrower than in Fig. 5b. The narrowness of the bands is a measure of the perfection of the crystallites constituting the phases. Figure 5d shows the Raman spectrum after further polishing. The diamond Raman line at 1331 cm^{-1} and the amorphous diamond-like carbon band have vanished completely, leaving the two graphite bands more pronounced than before. It is believed that the amorphous diamond-like carbon was completely converted into the nanocrystalline and microcrystalline graphite phases. The layers formed by the graphite phases are so thick that the diamond Raman line is extinguished. Further polishing for 16 h (Fig. 5e) washed the nanocrystalline and the microcrystalline graphite gradually from the surface of the diamond film down

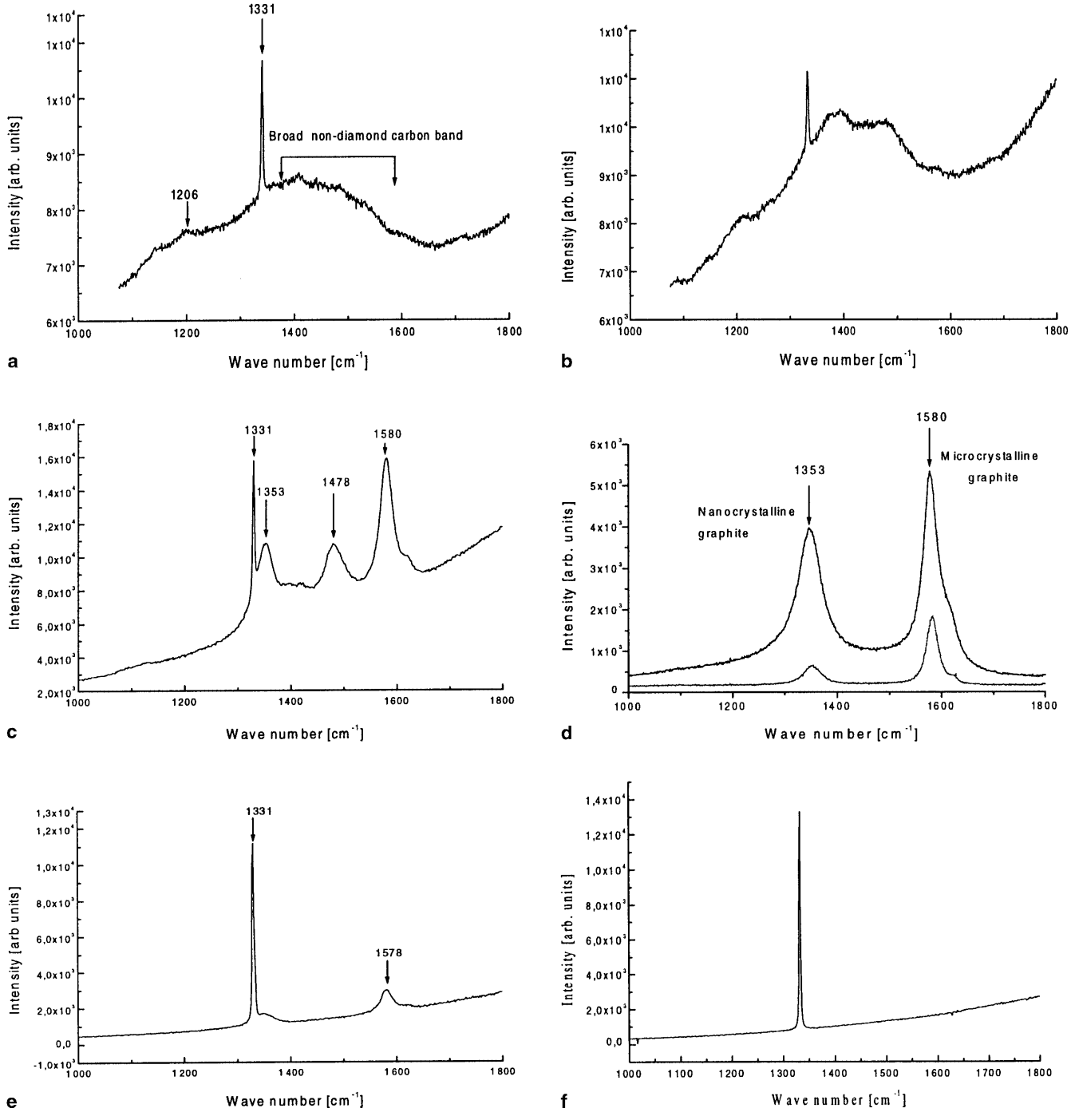

Fig. 5a–f Transformation of diamond into non-diamond carbon phases during thermochemical polishing. **a** Raman spectrum before polishing, showing non-diamond carbon phases. **b–f** Raman spectra at successive stages of polishing, showing pronounced non-diamond carbon phases and their subsequent vanishing by persistent polishing at intermittently reduced polishing temperatures

into the polishing plate through the process of diffusion of carbon atoms, so that in effect only a flimsy trace of the nanocrystalline graphite band and a small microcrystalline graphite band could be seen. The diamond Raman line at 1331 cm^{-1} is also reinstated, showing that the graphite layers have been thinned down below the penetration depth of the Ar^{+} laser used in the characterization. Figure 5f shows the Raman spectrum after a final fine-polishing at 750 °C and at moderate pressure. No traces of non-diamond phases could be seen. The intensity of the diamond Raman line at 1331 cm^{-1} is also increased considerably, manifesting the absence of a graphite layer on the surface of the polished diamond film. The diamond Raman line is seen to maintain its original position at 1331 cm^{-1} after polishing, indicating that thermochemical polishing does not distort the lattice structure of the surfaces on the diamond films [4].

Figure 6a shows the confocal Raman spectrograph of the intensities of the two graphite phases relative to the diamond Raman line intensity as function of depth. The measurement was done on the growth side of the diamond film at the stage of polishing shown in Fig. 5c. There are basically three distinct sections to be seen on the curves. Between 0 and 4 μm there is a steep rise in the relative intensity. This could be attributed to the high concentration of non-diamond phases in this range, which consequently leads to a sharp decrease in the diamond Raman line intensity with depth. A very abrupt fall in the relative intensity is observed, however, between 4 and10 μm. This shows that the concentrations of the graphite phases diminish rapidly with depth in this region. Above 10 μm, the change in intensity with depth is very minimal and the curves run almost parallel to the depth axis. This region is believed to be relatively free of graphite.

Fig. 6 **a** Depth distribution of disordered (nanocrystalline) graphite and microcrystalline graphite shown in Fig. 5c as function of the diamond Raman line. **b–d** Depth distribution of the two graphite phases as shown in Fig. 5d, taken with confocal Raman technique on three different spots on a thermochemically polished sample

The curves in Fig. 6b–d are confocal Raman spectrographs of the depth distribution of the intensities of the nanocrystalline graphite and the microcrystalline graphite phases at three different spots in the absence of the diamond Raman line shown in Fig. 5d. The measurements were also done on the growth side of the diamond film. The intensities of both phases are seen to drop rapidly within the first 5 μm. They drop more slowly in the next 5 μm and then run almost parallel to the depth axis. The curves in Fig. 6a–d are identical and their trend is a measure of the inverse phase purity of the diamond film. They clearly show that the first 10 μm of the film contains non-diamond carbon, while the film is relatively pure at depths above 10 μm. In effect, we have observed that the purity of a diamond film in the thermochemical polishing process increases with increasing distance from the surfaces of the film.

Photoluminescence spectrographic measurements were performed on both the as-grown films and on the films after polishing. The source of excitation was the 514.532 nm argon ion laser line. The region of photon energies ranging from 1.5 to 2.4 eV was investigated. The measurements were carried out at liquid nitrogen

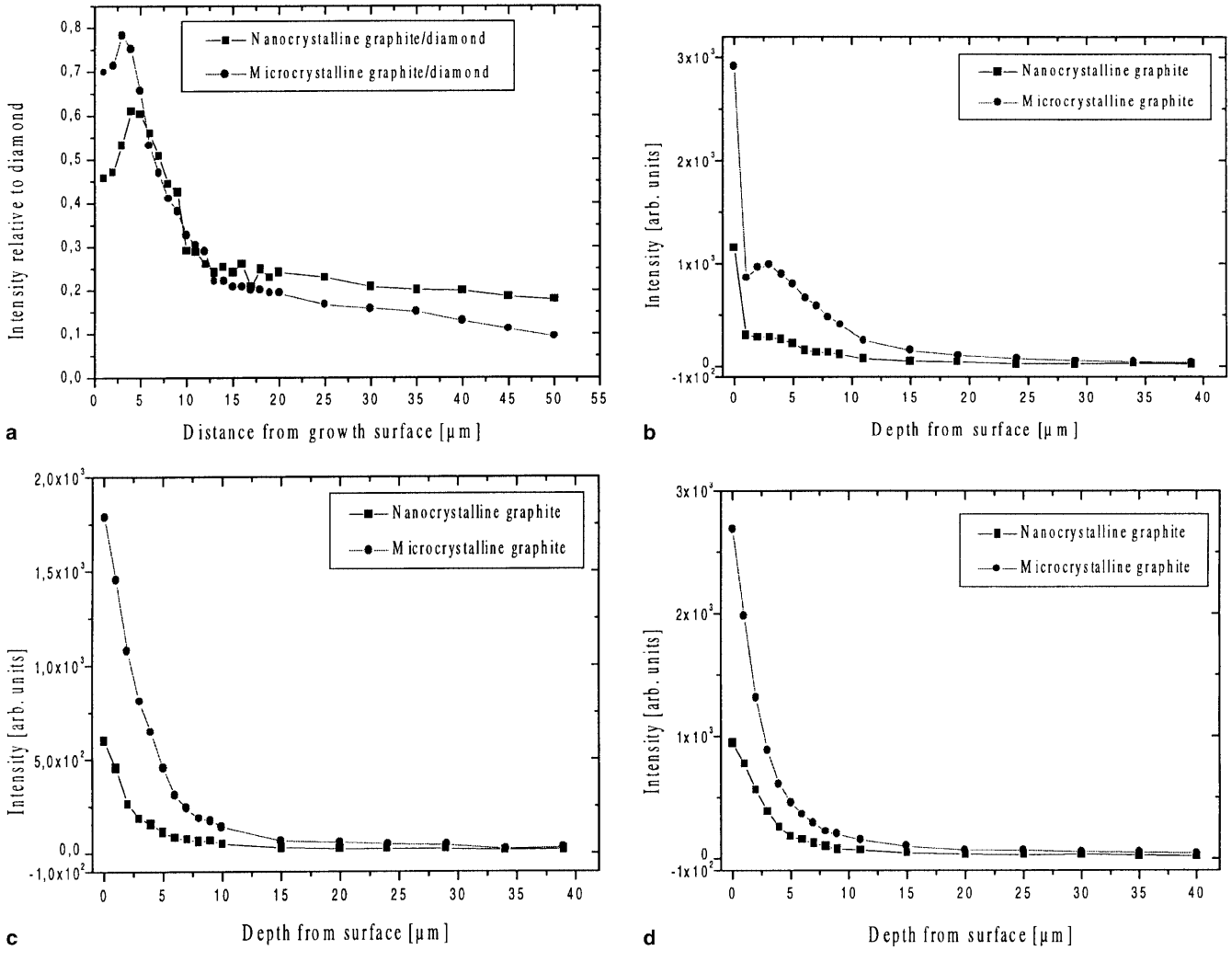

temperature, where a good signal-to-noise ratio can be attained.

The luminescence of defect centers depends on many parameters. The main ones are the concentration of the optically active defects, the excitation conditions, and the likelihood of radiative electronic transitions [22]. Figure 7 shows the photoluminescence spectra of defect centers for both the growth and substrate sides of an as-grown CVD diamond film. It can be observed that both sides of the film exhibit the same kind of defect centers with almost equal intensities. There are basically three zero-phonon bands in each spectrum followed by their respective phonon replicas. The phonon replicas result from the electron-phonon coupling on the optically active centers and the bands are formed through interactions with local vibrations, quasi local vibrations, and short wave acoustic phonons [22]. Several models have been proposed to discuss the zero-phonon line at 2.156 eV. One atomic model suggests that this defect center is due to the bonding of one single interstitial nitrogen atom to the nearest vacancy along the ⟨001⟩ axis [23, 24]. Another model assumes an association of vacancy and substitutional nitrogen atom in neutral charge state NV^0 [25, 26].

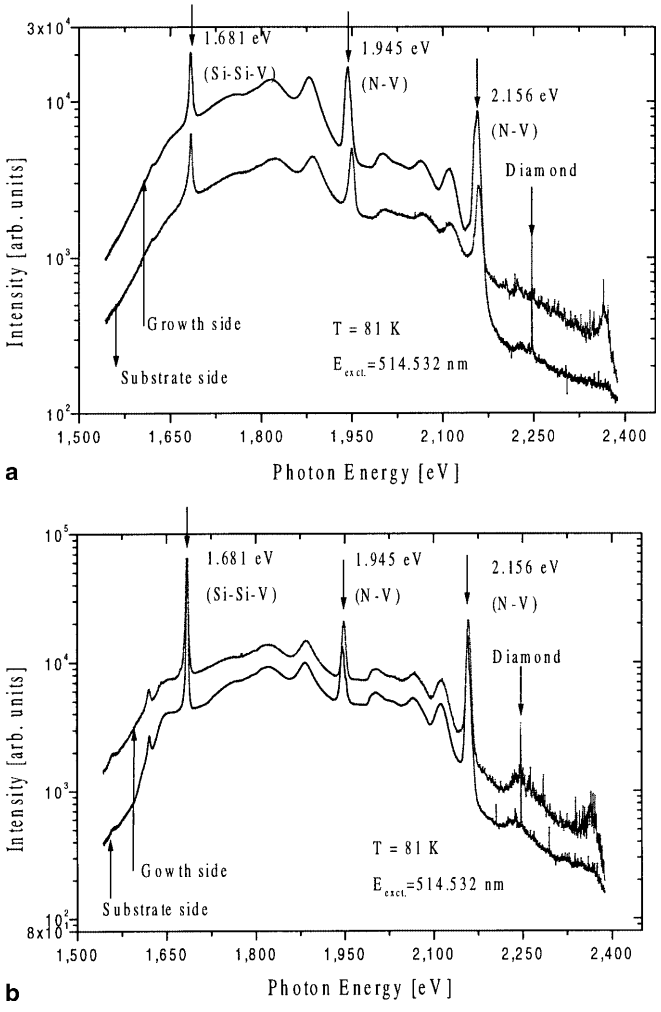

Fig. 7 Photoluminescence spectra of the growth and substrate sides of a CVD diamond film **a** as-grown and **b** after thermochemical polishing

There are clearly three phonon replica bands to be seen. The first two bands are attributed to acoustic phonons and the latter to optical phonons interacting with electronic transitions of the defect centers. The zero-phonon band at 1.945 eV consists of substitutional nitrogen atoms bound to the nearest vacancy filled with one electron (N-V defect) [27, 28]. This center may be the negatively charged N-V^- defect. The zero-phonon band at 1.681 eV results from a silicon-silicon-vacancy complex (Si-Si-V). The plasma interaction with silicon is believed to be the main reason for the formation of the Si center in the CVD diamond films [29]. Its phonon side bands are not as pronounced as those in the nitrogen defect centers. Figure 7b shows photoluminescence spectra of the same film as in Fig. 7a after thermochemical polishing. The spectra possess the same zero-phonon bands and phonon replica bands as the unpolished film. However, the phonons replicas of the silicon-vacancy complex are more pronounced after polishing, manifesting better structural quality of the polished surface.

Figure 8 shows the depth distribution of the defect centers in a polished diamond film examined by the confocal Raman method at three different spots on the film. The 2.156 eV and 1.945 eV complexes are fairly constantly distributed in the film. The silicon defect centers show a uniform distribution in the film as revealed by the curves of Fig. 8. One typical trend though, is that the Si-V complexes tend to be concentrated near the substrate side of the film, getting less from the center towards the growth side. This tendency is to be expected since silicon substrates were used to grow the films. Figure 8 also shows that the defects center extend from the substrate side to the growth side of the film, in accordance with the photoluminescence spectra shown in Fig. 7a and b.

Conclusion

The thermochemical polishing technique has been demonstrated to be effective in thinning the surface roughness of polycrystalline CVD diamond films to about 2.2 nm on both sides of the film. This has been done without encountering difficulties in specific planes and directions of the crystallites constituting the film. The efficient polishing of the substrate side was a consequence of the vibrational motor. Its transverse vibrations ensured that the weight meant to keep contact between the polishing plate and the film did not rotate during polishing. The mechanism of polishing is based on the transformation of diamond into non-diamond carbon and the subsequent dissolution of the carbon atoms into the metals constituting the upper weight and

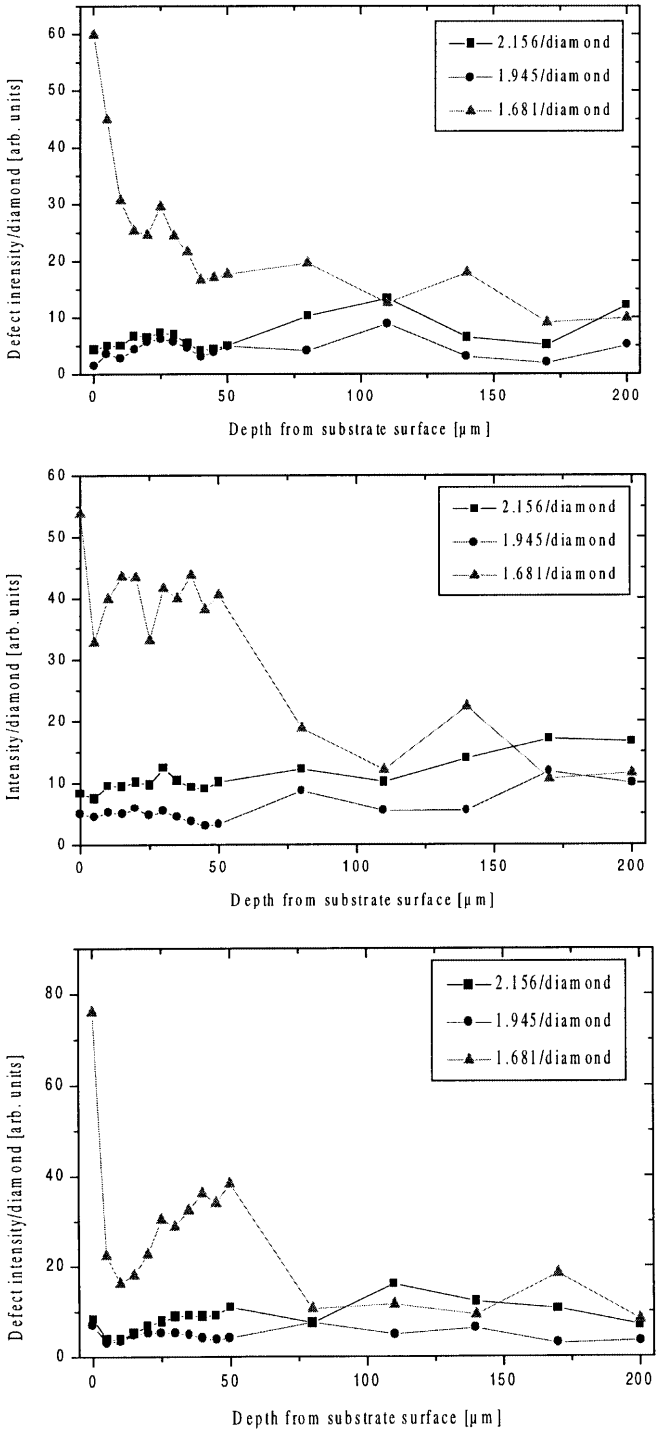

Fig. 8 Intensities of the defect centers relative to the diamond Raman line taken at three different spots on the substrate side of the sample

the polishing plate. Non-diamond carbon phases discovered during polishing included the nanocrystalline graphite at 1353 cm^{-1}, the amorphous carbon at 1453 cm^{-1} at the initial stage of polishing, and the microcrystalline graphite at 1580 cm^{-1} at the intermediate stage of polishing. The degradation of diamond into graphite at the polishing temperatures (700–900 °C) is attributed to transition metal enhanced graphitization of the diamond film. The constituent diamond phases vanished with persistent polishing. The grain boundaries of as-grown CVD diamond films contain non-diamond carbon phases which can be seen even before polishing. These phases appear to be more pronounced at the initial stages of polishing at higher temperatures. It is believed that the conversion of diamond into non-diamond carbon phases occur faster at higher temperatures, such as those used during the initial polishing of the films. However, polishing at lower temperatures showed that the diffusion rate is faster than the conversion of diamond into non-diamond phases. This was manifested by the gradual vanishing of the non-diamond phases as the polishing temperatures was intermittently reduced. Final polishing at 750 °C left the diamond surfaces completely free of non-diamond carbon phases, signifying that no non-diamond carbon phases exist at such low temperatures. Photoluminescence investigation of defect centers revealed three zero-phonon bands which represent the nitrogen-vacancy complexes at 2.156 eV and at 1.945 eV and the silicon-vacancy complex at 1.681 eV. Although the two nitrogen-vacancy complexes have equal atomic components (namely N-V), the difference in their energies is a result of the difference in their atomic structure or the difference in their charge states. The two nitrogen-vacancy complexes are distributed fairly uniformly in the films, while the silicon-vacancy complexes are concentrated in the proximity of the substrate side, showing a sparsely distributed tendency towards the growth side. The behavior is the consequence of the use of silicon as substrate during film growth.

Acknowledgements The authors express their sincere gratitude to Prof. Peter Koidl of the Frauenhofer Institute for Applied Solid State Physics in Freiburg, Germany, for supplying the CVD diamond films. They also gratefully acknowledge the financial assistance of the German Research Society (DFG) towards the project. Technical assistance rendered by the laboratory engineer Mr. Boguslaw Wdowiak is highly appreciated.

References

1. Chio SR, Jung DY, Kweon SY, Jung SK (1996) Thin Solid Films 279: 110
2. Yoshikawa M, Okuzumi F (1996) Surf Coat Technol 88: 197
3. Ramesham R, Rose MF (1998) Thin Solid Films 320: 223
4. Zaitsev AM, Kosaca G, Richarz B, Raiko V, Job R, Fries T, Fahrner WR (1998) Diamond Relat Mater 7: 1108
5. Van Enckevort WJP, Van Halewijn HJ (1994) Shaping of diamond. In: David G (ed) Properties and growth of diamond. INSPEC, London, p 293
6. Jin S, Zhu W, Groebner TE (1995) Techniques for diamond thinning and polishing by diffusional reactions with metals. In: Feldman A, Tzeng Y, Yarbrough WA, Yoshikawa M, Murakawa M (eds) 3rd international conference on applications of diamond films and related materials. NIST special publication 885, Gaithersburg MD, USA, p 209
7. Koslowski B, Strobel S, Wenig MJ, Martschat R, Ziemann P (1998) Diamond Relat Mater 7: 322
8. Okuzumi F, Yang CF, Yishikawa M (1995) Applications for precision cutting of sharpening CVD diamond film. In: Feld-

man A, Tzeng Y, Yarbrough WA, Yoshikawa M, Murukawa M (eds) 3rd international conference on applications of diamond films and related materials. NIST special publication 889, Gaithersburg, MD, USA, p 201
9. Okuzumi F, Yang CF, Yishikawa M (1995) Diamond Films Technol 4: 233
10. Yoshikawa M (1990) SPIE Proc Ser 1325: 210
11. Tokura A, Yang CF, Yoshikawa M (1992) Thin Solid Films 212: 49
12. Okuzumi F, Tokura H, Yoshikawa M (1994) Cutting performance of CVD diamond polished by thermo-chemical polishing method. In: Saito S, Fujimori N, Fukunaga O, Kamo M, Kobashi K, Yoshikawa M (eds) Advances in new diamond science and Technology. MYU, Tokyo, p 783
13. Grigoriev AP, Lifshits SC, Shamaev PP (1977) Kinet Catal 18: 948
14. Vishnevskii AS, Lysenko AV (1974) Synth Diamonds 4: 7
15. Phillips RW (1994) Surf Coat Technol 68/69: 770
16. Koslowski B, Strobel S, Wenig MJ, Marzschat R, Ziemann P (1998) Diamond Relat Mater 7: 322
17. Zhang Q, Yoon SF, Ahn J, Rusli, Guo YP (1998) Microelectron J 29: 875
18. Sails SR, Gardiner DJ, Bowden M, Savage J, Rodway D (1996) Diamond Relat Mater 5: 589
19. Vorlilek V, Rosa J, Vanecek M, Nesladek M, Stals L (1997) Diamond Relat Mater 6: 704
20. Grasselli JG, Buklin BJ (1991) Analytical raman spectroscopy. (Monographs on analytical chemistry and its applications, vol 114) Wiley, New York
21. Shiano S, Hoffman RW (1996) Thin Solid Films 283: 145
22. Zaitsev AM, Melnikov AA, Denisenko AV, Varichenko VS, Job R, Fahrner WR (1996) MRS Symp proc Ser 416: 113
23. Zaitsev AM, Uliyashin AG, Ali Noor H (1991) Superhard materials 1: 18
24. Ulyashin AG, Zaitsev AM, Ali Noor H (1992) Mater Sci Eng B11: 359
25. Mita Y (1996) Phys Rev B 53: 11360
26. Lawson SC, Fisher D, Hunt DC, Newton ME (1998) J Phys Condens Matter 10: 6171
27. Loubser JHN, Wyl JA (1978) Rep Prog Phys 41: 1210
28. Mainwood A (1994) Phys Rev 49: 746
29. Bergmann L, Stomer BR, Turner KF, Glass JT, Nemanich RJ (1993) J Appl Phys 73: 3951